Low-resistance magnetic tunnel junctions by in situ natural oxidation

H. Boeve, J. De Boeck, and G. Borghs

Citation: Journal of Applied Physics **89**, 482 (2001); doi: 10.1063/1.1328064
View online: http://dx.doi.org/10.1063/1.1328064
View Table of Contents: http://scitation.aip.org/content/aip/journal/jap/89/1?ver=pdfcov
Published by the AIP Publishing

Low-resistance magnetic tunnel junctions by *in situ* natural oxidation

H. Boeve, J. De Boeck, and G. Borghs
IMEC v.z.w., Kapeldreef 75, B-3001 Leuven, Belgium

(Received 21 March 2000; accepted for publication 29 September 2000)

Spin-dependent tunneling has received much attention in recent years. In this study, low-resistance exchange-biased magnetic tunnel junctions (down to 2 μm^2) were fabricated in a self-aligned way. The insulating barrier was achieved by *in situ* natural oxidation of very thin Al layers (<1.3 nm). The resistance and magnetoresistance of tunnel junctions is studied as a function of the aluminum thickness for different oxidation times, leading to resistance-area products from 0.1 to 5 k$\Omega\,\mu m^2$, and tunnel magnetoresistance (TMR) ratios up to 20%. The decrease in TMR for the lowest resistance barriers in the data set is explained by the nonuniformity of the initial Al layer, which has been characterized using different methods. In this case, the optimal oxidation state cannot be reached. The barrier oxidation state can be improved by thermal treatment, by which an increase in TMR is observed for temperatures up to 275 °C. © *2001 American Institute of Physics.*
[DOI: 10.1063/1.1328064]

I. INTRODUCTION

Spin-dependent transport in magnetic tunnel junctions leads to large magnetoresistance effects at room temperature as first demonstrated by Moodera.[1,2] This physical effect is likely to be exploited commercially in the short term, in magnetoresistive random access memory (MRAM), and read heads. Initially, the junction resistance was excessively high for these applications. The important considerations are the read and write speed which are set by the *RC* constants in the system. The requirements to be met for MRAM and read heads are 1 to 10 k$\Omega\,\mu m^2$ and below 100 $\Omega\,\mu m^2$, respectively.[3,4]

The tunnel barrier in ferromagnet-insulator-ferromagnet (FMIFM) trilayers is crucial to the resistance and the overall performance. To date, the best tunnel barriers are made by first depositing a thin Al precursor layer followed by an oxidation step. Several oxidation techniques have been explored to yield good magnetic tunnel junction properties. Plasma oxidation techniques are mostly used[1,5,6] but recently promising and reproducible results were obtained by *in situ* natural oxidation[7–9] and ultraviolet light assisted oxidation,[10,11] i.e., lower resistance-area products but moderate TMR values.

For plasma oxidized junctions the Al thickness was decreased below 1.0 nm in order to reduce the resistance-area product to an acceptable level. Quite contradictory, Mitsuzuka *et al.*[8] could reach similar resistance-area products starting from 2.0 to 3.0-nm Al in combination with *in situ* natural oxidation, while they observed a much smaller effective barrier thickness. In this article, we report on our study of *in situ* natural oxidation of ultrathin (<1.3 nm Al), freshly deposited Al layers between ferromagnetic layers to form low-resistance tunnel barriers. The observed transport measurements are related to the tunnel barrier properties as found from structural and magnetic analysis.

II. EXPERIMENTAL DETAILS

A set of magnetic tunnel junctions was prepared in a two-chamber ultrahigh vacuum sputter system, with a base pressure below 1×10^{-8} Torr. *In situ* natural oxidation of the thin Al layer was performed in the load-lock, which was filled with O_2 to reach a pressure of 100 Torr. The only parameter varied in this set of experiments was the oxidation time. After oxidation the introduction chamber was pumped down again, and the top electrode was deposited after sample transfer.

$Co_{90}Fe_{10}$–AlO_x–$Co_{90}Fe_{10}$–$Ni_{80}Fe_{20}$ multilayers were deposited at room temperature in a uniform in-plane magnetic field to induce a uniaxial magnetocrystalline anisotropy in the ferromagnetic layers. Starting from Si wafers covered with 50 nm thermally grown SiO_2, an exchange-bias scheme Ta 3 nm/NiFe 3 nm/FeMn 12 nm was included in the bottom electrode which is completed by 6-nm CoFe. The Ta/NiFe layer under the FeMn is a buffer layer to improve the (111) texturing in the γ-FeMn layer.[12] The initial Al thickness was varied between 0.4 and 1.3 nm. Using dc sputter power of 50 W for a substrate-target distance of 10 cm, the sputter rate is about 0.6 Å/s, resulting in effective sputtering times between 7.5 and 22.5 s. This provides us with a reproducible and noncritical timing scheme. The oxidation time was varied: 10 min, 1 h, or 12 h. After oxidation, the ''free'' top electrode is deposited and consists of 2 nm CoFe/8 nm NiFe and 5 nm Cu to prevent oxidation of the ferromagnetic layer.

Magnetic tunnel junction devices were achieved after a self-aligned, photolithographic processing[5] which consists of a double ion milling step to define bottom and top electrodes, followed by a self-aligned SiO_2 passivation step, by rf magnetron sputtering. A final metallization provides the contacting pads. After processing, the unidirectional exchange coupling is induced in the bottom electrode by a short anneal above the Néel temperature of FeMn (150 °C) and cooling down in an external magnetic field. All tunnel junction devices have a cross-type geometry, which allows four-point

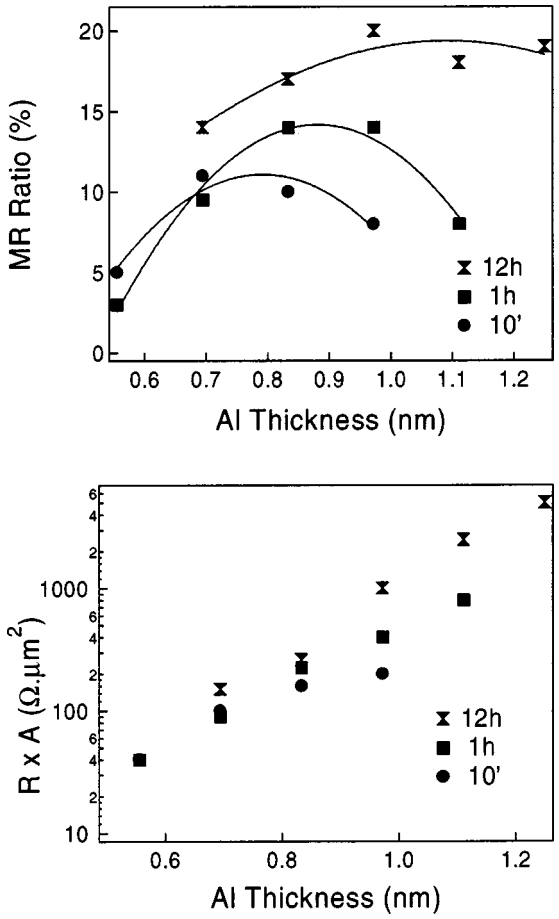

FIG. 1. Thickness dependence of TMR (a) and RA product (b) for a set of FeMn–CoFe–AlO_x–CoFe–NiFe tunnel junctions using different oxidation times (●:10 min, ■:1 h, ⧗:12 h). The symbols represent the experimental data points whereas solid lines are only guides to the eye.

resistance measurements. The device size is scaled from 100 μm by 100 μm down to 1 μm by 2 μm. Only the smallest junctions (<10 μm^2) were used in the data analysis. For larger devices an increase in tunnel magnetoresistance (TMR) was observed, which is due to the geometrical enhancement,[13] when the junction resistance becomes smaller than the bottom electrode sheet resistance, i.e., $R_{\square} = 20\ \Omega$. The voltage bias used in the resistance measurements was kept below 20 mV in order to exclude reduction in TMR caused by the voltage bias dependence.[2]

III. RESULTS

For all deposited CoFe–AlO_x–CoFe–NiFe junctions, the resistance and magnetoresistance properties can be related to the Al thickness before oxidation and the oxidation time. Figure 1(a) shows the magnetoresistance as a function of the Al thickness. All tunnel junctions with an initial Al thickness higher than 0.5 nm show TMR values of several percent at room temperature, while maximum TMR values up to 20% were measured for 12 h oxidation of 1.0 nm Al. The TMR ratio typically decreases to half its low-bias value at the voltage $V_{1/2}$ of 450 mV, which is in good agreement with reported values for other oxidation methods. In Fig. 1(a), all low-bias TMR values from the different samples and process runs were collected and solid lines were added as guides to the eye.

For all oxidation times the same trend is observed. A maximum TMR signal is found for the optimal Al thickness, for which all Al in the barrier is expected to be oxidized. For a thicker Al layer spin-flip scattering in the remaining unoxidized Al reduces the TMR, whereas for thinner Al, overoxidation will lead to oxidation in the bottom electrode and reduce the spin polarization at the ferromagnet-insulator interface. When comparing different oxidation times, the optimal Al thickness increases with oxidation time, and nicely fits the Cabrera–Mott theory on metal oxidation.[14] When comparing the oxidation times used in this study, the TMR at the optimum Al thickness decreases for shorter oxidation, which is an important issue for further investigation and discussion.

In Fig. 1(b) the junction resistance-area (RA) product is presented for the set of samples. In agreement with Simmons' theory for a rectangular tunnel barrier in metal-insulator-metal tunnel junctions,[15] the resistance increases exponentially with the Al thickness. The oxidation time only comes in as a second parameter for an Al thickness larger than 0.9 nm. Therefore we can conclude that below 0.9 nm the Al precursor in nearly instantly oxidized. For thicker Al layers the resistance increase saturates as the oxidation time was not sufficient to fully oxidize the Al layer. The saturation point for the different oxidation times coincides with the maximum TMR in Fig. 1(a).

Brinkman's formula[16] was used to fit the I–V and dI/dV–V curves in the voltage range of 0.2 to 1 V. The mean barrier height and effective thickness of the different samples were derived to be in the range of 2.2 to 2.5 eV and 0.6 to 0.8 nm, respectively. Moreover, the barrier asymmetry reflects either the incomplete oxidation of the barrier or the partial oxidation of the bottom electrode. For tunnel junctions with RA product under 100 $\Omega\ \mu m^2$, the expected barrier asymmetry disappears, which should be further addressed by investigating smaller (submicron) junctions in order to exclude any influence of the junction geometry.[13]

The tunnel barrier characteristics of overoxidized Al layers can be improved by annealing treatment. In Fig. 2 the evolution of the barrier resistance in the parallel and antiparallel magnetization state as well as the TMR value is shown as a function of the anneal temperature for an overoxidized 0.8-nm Al tunnel barrier (12 h oxidation time). Consecutive short anneal steps of 5 min were performed for increasing temperatures from 150 °C, i.e., the temperature used to induce the exchange bias, up to 300 °C. The tunnel barrier resistance linearly increases for both the parallel and the antiparallel state, or in other words the tunnel barrier itself is not degrading up to 300 °C. The TMR increases at 250–275 °C and reaches the maximum TMR value (20%) as found in thicker, optimal Al samples for 12 h oxidation time, and then starts to decrease at 300 °C. The junction switching behavior was not influenced during this annealing procedure.

For similarly prepared tunnel junctions with NiFe electrodes, see Fig. 2, the effect of annealing on the TMR is more pronounced. The higher initial resistance is due to dif-

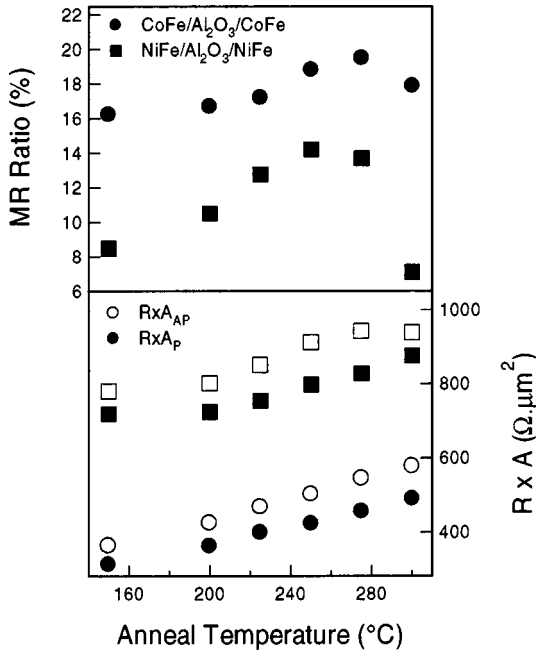

FIG. 2. Influence of the annealing temperature on R and TMR for tunnel junctions with CoFe or NiFe interfacial layers.

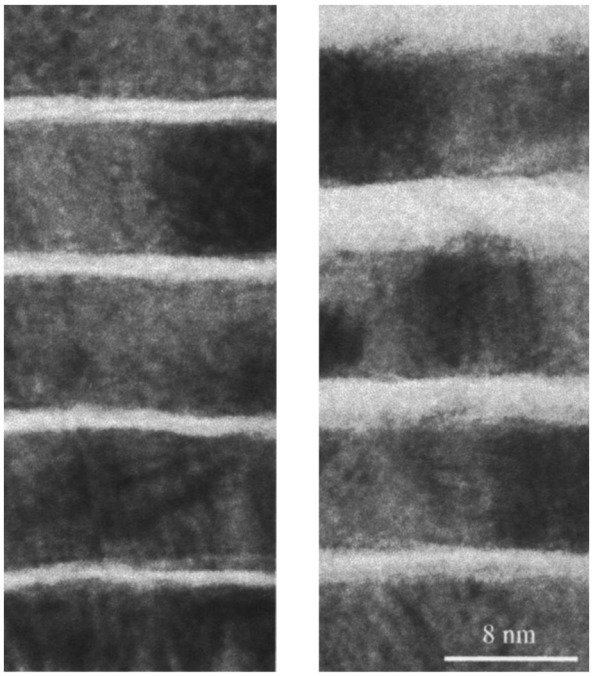

FIG. 4. Two TEM cross sections of Co/AlO_x multilayers. (a) Using *in situ* natural oxidation. (b) By reactive dc magnetron sputtering from an Al cathode.

ferent oxidation conditions, i.e., 20 h oxidation at 250 Torr. On the other hand, the increase of the tunnel barrier resistance is very similar to the case of CoFe electrodes. The mechanism responsible for the TMR increase upon annealing is believed to rely on the reorganization of oxygen atoms improving the interfacial quality,[6] hence the spin polarization of the ferromagnetic electrodes. The strong tunnel junction resistance increase upon annealing may rather be related to the reduction of inelastic spin-independent tunneling processes, e.g., trap-assisted tunneling,[17] since during annealing at elevated temperature, this trap density can be partially annihilated.

IV. DISCUSSION

When relating the TMR to the RA product for the set of CoFe–AlO_x–CoFe–NiFe tunnel junctions, as shown in Fig. 3, the TMR ratio is observed to be consistently lower for the smaller RA products. As very thin Al layers were oxidized to form a tunnel barrier, the uniformity of this layer is an important concern. The Al layer can be discontinuous, so that pinholes exist between both ferromagnetic layers. The reduction in magnetoresistance can then be explained from the competition between spin-dependent tunneling through the low-resistance insulating AlO_x layer, and ohmic conduction through the pinholes, where no AlO_x could be formed. But even for a continuous Al layer, a reduction in TMR can be predicted in the case of a nonuniform natural oxidation, such that the bottom electrode is locally oxidized while metallic Al is still present in the barrier. Hence the optimal barrier oxidation state cannot be achieved anymore.

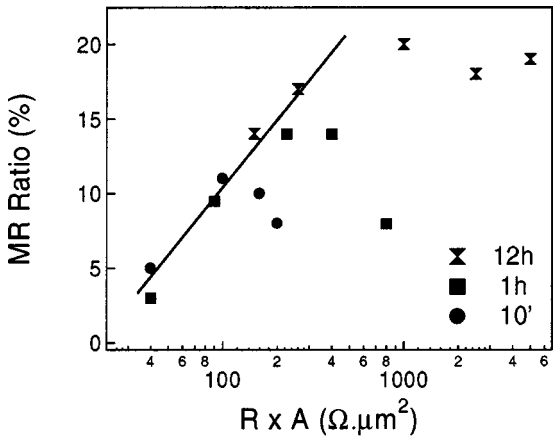

FIG. 3. TMR as function of RA product for the set of tunnel junctions.

More sensitive characterization techniques were utilized to explore the microscopic origin of the TMR decrease for low RA products. Therefore tunnel barriers formed by natural oxidation were studied using transmission electron microscopy (TEM) and x-ray photoelectron spectroscopy (XPS). By studying the interlayer coupling, the tunnel junction magnetoresistance curves can also reveal more information on the barrier uniformity.

In Fig. 4, the TEM cross section of two different Co/AlO_x multilayers is shown. The multilayers were grown on a thick Co/Ta buffer layer (not shown) on a Si substrate, from which the native oxide was not removed, to have a ''bottom electrode''-like metal thickness under the tunnel barriers. In Fig. 4(a), a multiple tunnel barrier was formed by natural oxidation of 0.8 nm (1 h oxidation) and three times 1.1 nm (1 h, 3 h, and 12 h oxidation) Al layers, each separated by 8 nm Co. The layer thickness resembles the grain size in the Co layers, since a new nucleation process is initiated onto the amorphous oxide layer. The tunnel barriers formed during the oxidation process are continuous and fol-

low the topography of the underlaying Co layer. The same observation was made for Co/Al (unoxidized) multilayers. After oxidation, the tunnel barrier thickness scales with the initial Al thickness rather than with the oxidation time, as the 0.8-nm Al barrier is noticeably thinner than the similar 1.1 nm Al barriers. During oxidation the real barrier thickness is increased by approximately 30% as compared to the initial Al thickness.

In comparison, in Fig. 4(b), the tunnel barriers were prepared by reactive dc magnetron sputtering from an Al target, in a 15% O_2/Ar ambient.[18] The oxygen is delivered at the substrate in order to shift the oxidation of the cathode to a higher oxygen partial pressure. Moreover, sputtering from an oxidized cathode would result in a strong decrease of the deposition rate. The TEM cross section reveals why no tunnel magnetoresistance was found in these layers: a strong oxidation of the ferromagnetic under the tunnel barriers can be observed. During the initial stage of the barrier deposition, the ferromagnet is unprotected and can obviously be oxidized. Therefore the oxidation is similar for different barrier thicknesses. A possible solution here would be to first deposit a thin Al layer to protect the ferromagnet underlayer.

For the *in situ* natural oxidation though, any bottom electrode oxidation could not be distinguished in the TEM images. In other words, overoxidation, if any, is expected to be limited to the first atoms in the bottom electrode. When relating the barriers in Fig. 4(a) to the magnetoresistance data in Fig. 1, the 0.8-nm Al barrier is close to the optimal thickness for 1 h oxidation time, but only shows 11% TMR. For the 1.1-nm Al barrier, 12 h oxidation time is optimal (20% TMR) but 1 h is insufficient and resulted in a strong decrease in TMR. Unfortunately, the TEM image only reveals minor contrast differences in the different tunnel barriers, which may be related to a difference in oxygen incorporation in the barrier. Anyhow, the 0.8-nm Al barrier does not appear to be as uniform as the others.

The uniformity of the Ar layer was further addressed by XPS. A series of Co/Al samples with varying Al thickness were deposited. Sample transfer between the two systems implies a vacuum break, which leads to an at least partly oxidized Al top layer. The Al thickness ranges from 0.7 to 1.6 nm. For the thicker Al layers a longer sample transfer time was allowed.

Al always appears to be oxidized after sample transfer, except for a 1.6-nm layer where a very small metallic peak was observed, which implies that unoxidized Al is left over in the barrier. In other words, the oxidation front did not reach the bottom electrode. In order to analyze possible oxidation of the Co bottom electrode, the Co $2p_{3/2}$ peak was also monitored. Two different peaks can be seen in the spectra in Fig. 5 at binding energies around 781 eV and 778 eV. The main peak at 778 eV can be attributed to metallic Co and the chemical shift in Co–O bonds in oxidized Co creates a second peak. Very small amounts of oxidized Co are difficult to observed in the naturally asymmetric Co *2p* peak. However, in the spectra for different Al thickness, we observe that the 0.7-nm Al layer leads to a well noticeable oxidation of the Co underlayer. The abruptness of this transient implies that for the oxidation times used, below 0.8-nm Al, bottom electrode oxidation must be strongly considered for any oxidation time, whether pinholes exist or not.

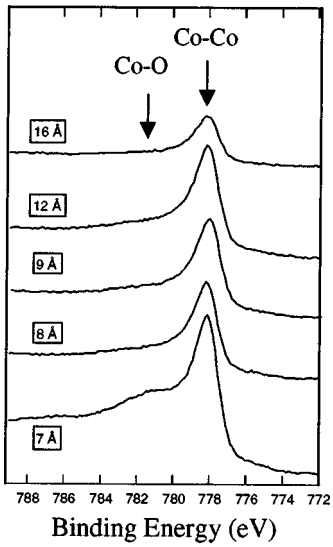

FIG. 5. The barrier oxidation process was studied by *ex situ* XPS. A continuous Al layer is obtained after 0.8-nm Al deposition as no trace of CoO_x is found in the XPS curves after the *ex situ* transfer. Only for an Al thickness of 1.6 nm was metallic Al still found.

From a magnetic point of view, the barrier smoothness can be studied from the magnetic coupling phenomena in the two ferromagnetic layers. In Fig. 6 the full magnetoresistance loop of a FeMn–CoFe–AlO_x–CoFe–NiFe tunnel junction (6×1 μm^2) is shown. In the graph two important coupling fields are indicated. The FeMn exchange-bias layer is responsible for the large shift in the switching field of the pinned layer, which is labeled as the exchange coupling field H_{exch}. An exchange field of 200 Oe is measured in the junctions with bottom electrode Ta 3 nm/NiFe 3 nm/FeMn 12 nm/CoFe 6 nm. Due to this exchange coupling, the magnetization vectors in the ferromagnetic layers are aligned fully antiparallel in the high resistance plateau region. The other resistance transition in Fig. 6 coincides with the free layer switching, and reveals that the free layer hysteresis loop is also shifted, which is labeled by the interlayer coupling field

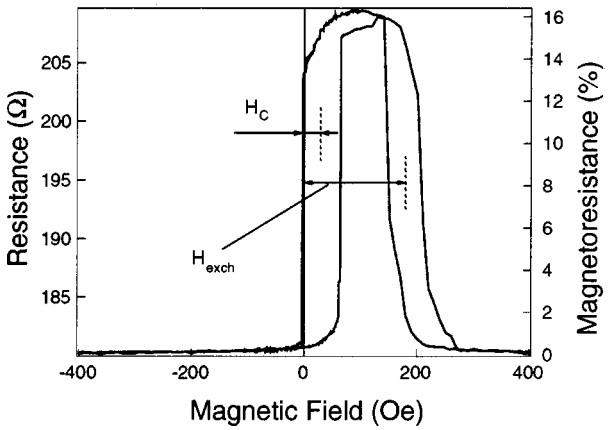

FIG. 6. Magnetoresistance loop from a FeMn–CoFe–AlO_x–CoFe–NiFe tunnel junction (6×1 μm^2). Schematically shown are the coupling fields present in the device.

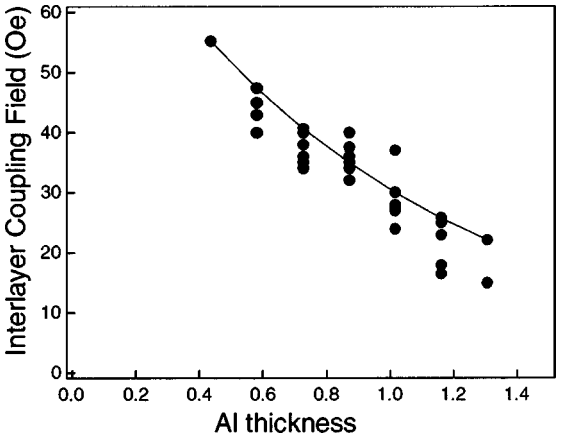

FIG. 7. Evolution of the coupling field H_C versus the Al thickness. The true AlO_x thickness in the model is estimated from bulk values for Al and Al_2O_3 to be 30% larger due to the incorporation of oxygen in the Al lattice, as was confirmed by TEM (see Fig. 4).

H_C. This magnetostatic coupling was first described by Néel[19] as being caused by the waviness of the magnetic layers in nonideal films, and is better known as ''orange-peel coupling.'' The coupling energy J is calculated from the two ferromagnetic films with saturation magnetization M and M', separated by a spacer layer with thickness t_{sp}, which have a two-dimensional sinusoidal waviness with amplitude h and wavelength δ, and is given as[20]

$$J=\frac{\pi^2}{\sqrt{2}}\frac{h^2}{\lambda}(\mu_0 M M')\exp\left(\frac{-2\pi\sqrt{2t_{sp}}}{\lambda}\right). \quad (1)$$

The coupling field H_C of the free layer (with thickness t_f) is then found as

$$H_C=J/(\mu_0 M t_F). \quad (2)$$

The interlayer coupling data obtained from the magnetoresistance loops in the sample set was fitted using Eq. (2) and is shown in Fig. 7. The saturation magnetization of CoFe is 1450 emu/cm^3, and the bilayer (CoFe–NiFe) free-layer thickness is recalculated by weighing the saturation magnetization of NiFe to CoFe. The true AlO_x thickness is estimated from bulk values for Al and Al_2O_3 to be 30% larger due to the incorporation of oxygen in the Al lattice, as was confirmed by TEM (see Fig. 4). The best fit parameters obtained are $h=0.22$ nm and $\lambda=12.5$ nm. The physical origin of these parameters can be related to the grain size (λ) and the tunnel barrier thickness variation (h), which may arise at the grain size boundaries. An extensive study using high-resolution transmission electron microscopy analysis of the junction cross section may reveal more details on the microscopic origin, but falls beyond the presented study.

The quality of the Al precursor layer is of extreme importance in the comparison between different tunnel junction fabrication procedures. As discussed before, Mitsuzuka *et al.*[8] showed TMR effects and similar resistance-area products using *in situ* natural oxidation, but only starting from 2.0 to 3.0 nm Al. Below 2.0 nm, the TMR decreases very fast. In this work, the bottom electrode roughness was first minimized, yielding roughness values at the barrier below 0.2 nm (rms, measured by AFM over an area of 1 μm^2), which is in good agreement with the analysis of the orange-peel coupling in the data set. On the other hand, we found using XPS that 0.8 nm Al is sufficient to fully cover, and initially prevent the oxidation of, the bottom electrode. Hence for these thin tunnel barriers, any bottom electrode roughness will quickly lead to local variations in the tunnel barrier thickness and, due to the exponential dependence of the tunnel current on the thickness, to hot spots where the majority of the current flows. Furthermore, local oxidation of the bottom electrode is expected at first in those points, resulting in a strong decrease of the TMR in the thinnest tunnel barriers.

Summarizing all evidence, the universal decrease in TMR for the lowest resistance barriers in the data set is caused by the Al layer nonuniformity. Since in this case the optimal oxidation state, where the Al is completely oxidized while the bottom electrode is still unoxidized, can most probably not be reached anymore. Hence a suboptimal situation is created where the bottom electrode is already being oxidized while the barrier is being formed. A nonuniform tunnel current distribution may further reduce the tunnel magnetoresistance.

V. CONCLUSION

Low-resistance exchange-biased tunnel junctions (down to 2 μm^2) were fabricated by *in situ* natural oxidation of very thin Al layers ($<$1.3 nm). The resistance and magnetoresistance of the junctions were studied as a function of the aluminum thickness for different oxidation times, leading to low resistance-area products between 0.1 to 5 kΩ μm^2 and TMR ratios up to 20%.

For the lowest resistance barriers the influence of the oxidation time is limited by the fast oxidation of the first monolayers of Al. The decrease in TMR values for these barriers is explained by the Al layer nonuniformity. Hence the optimal oxidation state cannot be realized anymore. Moreover, the largest contribution in the tunnel current is expected where the bottom electrode is locally oxidized. In this case, the oxidation state can be improved by thermal treatment.

ACKNOWLEDGMENTS

The authors are grateful to E. Vandeplas for help in processing, T. Conard and K. Attenborough for the XPS and AFM measurements, and P. Roussel and H. Bender for the TEM imaging. H.B. wishes to thank the IWT-Flanders for the financial support in the form of a scholarship.

[1] J. S. Moodera, L. R. Kinder, T. M. Wong, and R. Meservey, Phys. Rev. Lett. **74**, 3273 (1995).
[2] J. S. Moodera, J. Nassar, and G. Mathon, Annu. Rev. Mater. Sci. **29**, 381 (1999).
[3] H. Boeve, C. Bruynseraede, J. Das, K. Dessein, G. Borghs, J. De Boeck, R. C. Sousa, L. V. Melo, and P. P. Freitas, IEEE Trans. Magn. **35**, 2820 (1999).
[4] R. Coehoorn, S. R. Cumpson, J. J. M. Ruigrok, and P. Hidding, IEEE Trans. Magn. **35**, 2586 (1999).
[5] W. J. Gallagher, S. S. P. Parkin, Y. Lu, X. P. Bian, A. Marley, K. P. Roche, R. A. Altman, S. A. Rishton, C. Jahnes, T. M. Shaw, and G. Xiao, J. Appl. Phys. **81**, 3741 (1997).

[6] R. S. Sousa, J. J. Sun, V. Soares, P. P. Freitas, A. Kling, M. F. da Silva, and J. C. Soares, Appl. Phys. Lett. **73**, 3288 (1998).
[7] H. Tsuge, T. Mitsuzuka, A. Kamijo, and K. Matsuda, Mater. Res. Soc. Symp. Proc. **517**, 87 (1998).
[8] T. Mitsuzuka, K. Matsuda, A. Kamijo, and H. Tsuge, J. Appl. Phys. **85**, 5807 (1999).
[9] K. Matsuda, A. Kamijo, T. Mitsuzuka, and H. Tsuge, J. Appl. Phys. **85**, 5261 (1999).
[10] P. Rottländer, H. A. M. de Gronckel, H. Kohlstedt, E. Girgis, J. Schelten, and P. Grünberg, J. Magn. Magn. Mater. **210**, 251 (2000).
[11] H. Boeve, E. Girgis, J. Schelten, J. De Boeck, and G. Borghs, Appl. Phys. Lett. **76**, 1048 (2000).
[12] K.-M. H. Lenssen, A. E. M. De Veirman, and J. J. T. M. Donkers, J. Appl. Phys. **81**, 4915 (1997).
[13] R. J. M. van de Veerdonk, J. Nowak, R. Meservey, J. S. Moodera, and W. J. M. de Jonge, Appl. Phys. Lett. **71**, 2839 (1997).
[14] N. Cabrera and N. F. Mott, Rep. Prog. Phys. **12**, 163 (1948).
[15] J. G. Simmons, J. Appl. Phys. **34**, 1793 (1963).
[16] W. F. Brinkman, R. C. Dynes, and J. M. Rowell, J. Appl. Phys. **41**, 192 (1970).
[17] J. Zhang and R. M. White, J. Appl. Phys. **83**, 6512 (1998).
[18] H. Boeve, Ph.D. thesis, Katholieke Universiteit Leuven, 2000.
[19] L. Néel, Comptes Rendus **255**, 1676 (1962).
[20] J. C. S. Kools, IEEE Trans. Magn. **32**, 3165 (1996).